

Monoenergetic nuclear gamma rays were used to measure the resolution and pulse-height distribution for the complete spectrometer, the intrinsic efficiency of the crystal at different energies was calculated by numerical integration using the absorption coefficients compiled by White,⁷ the external absorption in this nonideal geometry was calculated by numerical integration, and the escape of the iodine x-rays was accounted for using the information of Axel.⁸ Application of the above information yielded a photon distribution which is believed reliable down to an energy of less than 80 keV; at lower energies the absorption and other effects give large corrections.

In Fig. 1 the transformed experimental points are compared to a spectrum calculated from the theory of Glauber and Martin for allowed electron capture transitions. Curves of the separate contributions by the 1S, 2S, and 2P shells to the theoretical spectrum are also shown. The relativistic corrections of Glauber and Martin and screening corrections of Brysk and Rose⁹ were applied.

⁷ G. R. White (unpublished).

⁸ P. Axel, Brookhaven National Laboratory Report BNL-271 (unpublished).

⁹ H. Brysk and M. E. Rose, Oak Ridge National Laboratory Report ORNL-1830 (unpublished).

Best fit between theory and experiment was obtained with an end-point energy of 320 keV for the 1S spectrum.

The variation of fit with maximum energy, together with a consideration of experimental errors, led to an estimate of ± 10 keV as a probable error. The energy measurement is in agreement with the value of 320 ± 10 keV of Saraf, who analyzed his data assuming a Morrison-Schiff¹⁰ spectrum, which does not include the large 2P contribution. The energy end point of 320 ± 10 keV would lead to a total disintegration energy of 355 ± 10 keV, taking into account the 1S shell binding energy of the daughter.

The fit with the predictions of the Glauber-Martin calculations is considered to be good within the accuracy of the experiment.

ACKNOWLEDGMENTS

Acknowledgment is made to Miss Joyce P. Davis for her assistance in taking some of the data and in the calculations.

¹⁰ P. Morrison and L. I. Schiff, Phys. Rev. **58**, 24 (1940).

Angular Distributions of the Gamma Rays from the Reaction $\text{Na}^{23}(p, \gamma)\text{Mg}^{24}\dagger$

F. W. PROSSER, JR.,*† N. P. BAUMANN,*§ D. K. BRICE, W. G. READ, AND R. W. KRONE
Department of Physics, University of Kansas, Lawrence, Kansas

(Received May 23, 1956)

Resonances occurring in the compound nucleus Mg^{24} resulting from the proton bombardment of sodium have been studied in the energy range from $E_p = 0.58$ to $E_p = 1.50$ MeV. Ten resonances were found to have a relatively large yield of capture gamma rays. The cascades leading to the ground state of Mg^{24} were determined and found to proceed for the most part through well-known lower lying states. The angular distribution of the first gamma ray emitted in the decay was measured for six of these resonances. The resonance energies in MeV and the corresponding assignments for spin and parity are the following: $E_p = 0.595, 0.676, 0.740, 0.744, 0.877$ (1+), 0.989 (4±), 1.022 (2-), 1.321 (3+), $1.398, 1.419$ (4+).

INTRODUCTION

THE proton bombardment of Na^{23} has long been known to give rise to gamma radiation, and as early as 1941 Burling¹ had discovered a number of resonances corresponding to highly excited states in Mg^{24} . Since then a rapidly increasing amount of information about the compound states has been collected

by various investigators.²⁻⁹ More recently, the study of the elastic scattering of alpha particles from Ne^{20} has added considerable information about those compound states in Mg^{24} that may be reached by this particular

† This research was supported in part by the Office of Naval Research and the National Science Foundation.

* National Science Foundation Predoctoral Fellow.

† Now at Rice Institute, Houston, Texas.

§ Now at Savannah River Laboratory, Augusta, Georgia.

¹ R. L. Burling, Phys. Rev. **60**, 340 (1941).

² P. M. Endt and J. C. Kluyver, Revs. Modern Phys. **26**, 95 (1954).

³ P. H. Stelson and W. M. Preston, Phys. Rev. **95**, 974 (1954); P. H. Stelson, Phys. Rev. **96**, 1584 (1954).

⁴ H. Casson, Phys. Rev. **89**, 809 (1953).

⁵ O. H. Turner, Australian J. Phys. **6**, 380 (1953).

⁶ Teener, Seagondollar, and Krone, Phys. Rev. **93**, 1035 (1954).

⁷ Grant, Rutherglen, Flack, and Hutchinson, Proc. Phys. Soc. (London) **A68**, 369 (1955).

⁸ J. O. Newton, Phys. Rev. **96**, 241 (1954).

⁹ J. Seed, Phil. Mag. **44**, 921 (1953).

process.¹⁰ Unfortunately the region of the compound nucleus investigated in this latter study does not overlap that region over which the most careful study of the $\text{Na}^{23} + p$ reactions had been previously carried out. Because of the uncertainties in the resonance energies and in the Q value of the reaction $\text{Na}^{23}(p,\alpha)\text{Ne}^{20}$, no definite matching of the two groups of states has so far been possible.¹¹ The present investigation was motivated in part by the hope that a more careful study of the $\text{Na}^{23} + p$ reaction at low bombarding energies would provide agreement with the results obtained from the $\text{Ne}^{20}(\alpha,\alpha)$ reaction.

At the same time, we have endeavored to study more thoroughly those resonances for which the capture process predominates. An intensive investigation of the decay spectra and the angular distributions of the most energetic gamma ray of the cascades may lead to spin and parity assignments for some of the compound states. Such information may be compared with or serve to supplement, similar assignments obtained from other reactions.^{12,13}

EXPERIMENTAL PROCEDURE

The University of Kansas electrostatic accelerator¹⁴ was used as the source of monoenergetic protons. The control signal to the corona load stabilizing the accelerator voltage is derived from analysis of the molecular beam by a 30° electrostatic analyzer. The energy resolution of the proton beam is better than 1 keV and data points were found to be reproducible to within 250 volts over short periods of time. The energy calibration was based on the resonances in the reactions $\text{Al}^{27}(p,\gamma)\text{Si}^{28}$ at 993.3 keV and $\text{F}^{19}(p,\alpha\gamma)\text{O}^{16}$ at 873.5 and 935.3 keV.¹⁵

Gamma radiation was detected with scintillation counters using DuMont 6291 or RCA 6199 photomultiplier tubes and NaI(Tl) crystals polished and sealed in an Argonne-type crystal mount.¹⁶ Because of the very low yields of the capture radiation, considerable care was necessary to minimize the background both from

the accelerator and from target contaminations. Satisfactorily clean targets were prepared by allowing a dilute solution of chemically pure NaOH to evaporate on a tungsten backing that had been previously cleaned by heating to a white heat in vacuum. Background not arising at the target was considerably reduced by placing lead shielding around the scintillation detectors, so that a minimum of 2 in. of lead was between the crystal and any extraneous source of radiation.

It is well known that the Mg^{24} compound nucleus, when formed by the proton bombardment of Na^{23} , may decay into five exit channels (Fig. 1). Three of these (p' , α' , and capture) lead to gamma-radiation characteristic of their particular mode of decay. The excitation curves for each of these reactions may be obtained separately, if the amplified output of a single counter enters three integral discriminators whose biases are set to accept all pulses corresponding respectively to gamma rays of energy greater than 0.3 MeV, 0.8 MeV, and 1.9 MeV. The high-energy gamma rays then correspond to the capture process, the medium-energy gamma rays (after subtraction of the high-energy gamma rays) to the α' channel, and the low-energy gamma rays (after subtraction of the medium- and high-energy gamma rays) to the p' channel. This was the method used by Stelson and Preston⁸ in their extensive study of the α' and p' channels. The present measurements confirm their results in the region of overlap but extend them by including the excitation curve for the capture process.

At those resonances at which a relatively large yield of high-energy gamma radiation was found to exist, a pulse-height analysis of the gamma-ray spectrum was obtained by using a single-crystal scintillation spectrometer. Any attempt to improve the resolution of the spectrum by employing two- or three-crystal spectrometers proved impractical because of the low cross section of the capture process. A simple technique for recording such a pulse-height distribution consists in feeding the amplified pulses from the counter into a pulse-lengthening circuit which gives a square-topped, 10-microsecond-long pulse whose amplitude is the same as the amplitude of the incoming pulse. This pulse is then displayed on the x axis of a DuMont Model 248 A oscilloscope. The original pulse is also used to trigger a blocking oscillator whose output signal is passed through a 2.5-microsecond delay line onto the intensifier to brighten the oscilloscope trace. The result is a sequence of bright dots whose displacement along the x axis is proportional to the pulse height of the detector output. These dots were photographed on a continuously moving film strip with a Fairchild Oscillo-Record camera. Following development, the film was placed into a photographic enlarger where the displacements of the dots from the base line were measured by dividing the film into a convenient number of channels and counting the dots in each channel. Energy calibration points were obtained by

¹⁰ Goldberg, Huberti, Galonsky, and Douglas, Phys. Rev. **93**, 799 (1954).

¹¹ Donahue, Jones, McEllistrem, and Richards, Phys. Rev. **89**, 824 (1953).

¹² Spin and parity assignments for a number of compound states have been made by Stelson⁸ by studying the angular distribution of the alpha particles in the $\text{Na}^{23}(p,\alpha)\text{Ne}^{20}$ reaction and by Goldberg *et al.*¹⁰ from an investigation of alpha particles elastically scattered by Ne^{20} . More recently, some assignments have been published by Newton⁸ and Seed.⁹ Many of the resonances found in the gamma-ray yield curves have also been observed at this laboratory by studying the elastic scattering of protons from Na^{23} .¹³ Spin and parity assignments made as a result of these experiments will be found in a later publication. It is of interest to note that at least one of the resonances ($E_p = 0.989$ MeV) is observed only in the capture process.

¹³ Baumann, Prosser, and Krone, Phys. Rev. **100**, 1244 (1955); Baumann, Prosser, Read, and Krone, Phys. Rev. **104**, 376 (1956), following paper.

¹⁴ L. W. Seagondollar, Final Report, ONR Contract No. 260-2, December 31, 1954 (unpublished).

¹⁵ Herb, Snowden, and Sala, Phys. Rev. **75**, 246 (1949).

¹⁶ R. K. Swank and J. S. Moenick, Rev. Sci. Instr. **23**, 502 (1952).

recording the 0.66-Mev gamma ray from Cs^{137} , the 1.63-Mev gamma ray from the $\text{Na}^{23}(p,\alpha\gamma)\text{Ne}^{20}$ reaction, the 6.12-Mev gamma ray from the $\text{F}^{19}(p,\alpha\gamma)\text{O}^{16}$ reaction, and the 9.7- and 12.8-Mev gamma rays resulting from the proton bombardment of thick boron targets.

In the energy range examined, ten resonances had a sufficient yield of high-energy gamma rays to justify a more detailed study of the decay. Of these, the spectra of four were considered to be too complex to provide unambiguous information from the angular distribution of the most energetic gamma ray in the cascade. For each of the other six, the angular distribution of the highest energy gamma ray was determined by comparing the yield as a function of the angular position of a movable counter to that in a monitor counter. The use of a monitor counter rather than a beam-current integrator as a reference was necessary because the long running times, required to obtain sufficient statistical accuracy, made the danger of target depreciation and drifts in accelerator voltage too great.

The target chamber was constructed with cylindrical symmetry about the target position. Inside was a small quartz plate provided with fiducial marks that could be pivoted in front of the target to check the beam alignment. The size of the beam was determined by a $\frac{1}{4}$ -in.-diameter aperture in a tantalum plate located several feet in front of the target. The movable counter was pivoted about a bushing through which the shaft of the target holder passed, thereby insuring the concentricity of the counter location with respect to the target. The 20-mil tungsten target backings were sufficiently thick to cause appreciable absorption at angles close to the plane of the target. The error due to this effect was reduced to less than $\frac{1}{2}\%$ by placing absorbers in front of the movable counter to maintain an almost constant thickness of tungsten between the target and detector at all angles. The solid angle subtended by the counter was determined by a $\frac{5}{8}$ -in.-diameter aperture in the 2-in.-thick lead shielding surrounding the counter. For the geometrical arrangement used, this corresponded to a maximum angular spread of 7 degrees.

The discriminator bias for the movable counter was set to accept only the most energetic gamma rays in the cascade, while that for the monitor counter was set considerably lower. Thus, the statistical accuracy of the measurements depended primarily on the counting rates in the movable counter. The various angles were run consecutively in one direction and then in reverse to reduce any error arising from drift in the discriminator settings.

The geometry of the experimental arrangement was checked by measuring the angular distribution of the gamma rays from the 0.935-Mev resonance in the $\text{F}^{19}(p,\alpha\gamma)\text{O}^{16}$ reaction, which is known to be isotropic.¹⁷

¹⁷ S. Devons and M. G. N. Hine, Proc. Roy. Soc. (London) **A199**, 56, 73 (1949).

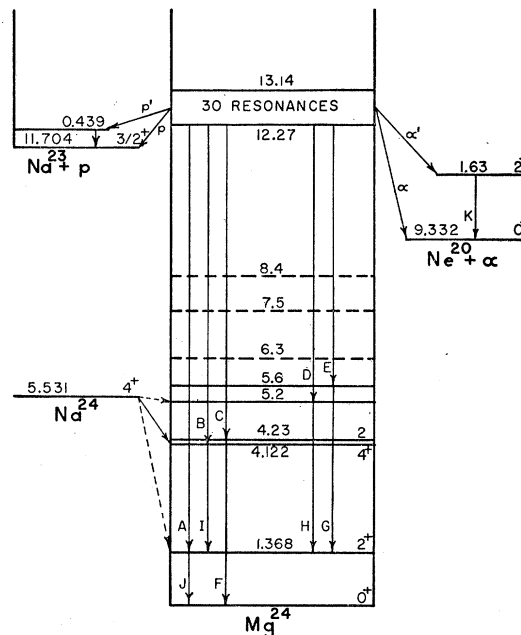


FIG. 1. Energy level diagram of Mg^{24} indicating the region of the compound nucleus surveyed in this investigation, the gamma-ray transitions observed, and the particle exit channels available.

The results of this check run have been included in Fig. 4.

EXPERIMENTAL RESULTS

The gamma-ray yields for the three reactions are shown in Fig. 2. The insert shows the two prominent resonances in the reaction $\text{F}^{19}(p,\alpha\gamma)\text{O}^{16}$. It is apparent from the relative yields and the half-widths that the two resonances at the same energies in the Na^{23} yield curve must almost entirely be due to the presence of fluorine contamination. This was also evident from the gamma-ray spectrum observed at these two resonances. The "tail" on the 0.873-Mev resonance appears, however, to be the result of a compound state in Mg^{24} . Such an identification was possible from the gamma-ray spectrum at that energy. The very low yield of capture radiation is evident from the scale. The numbers appearing in the diagram designate the various resonances observed in Mg^{24} . Several of these decay through the p and α channels only, which is the reason for their absence in the gamma-ray yield curve.¹⁸ In an earlier report¹⁸ it was erroneously stated that several resonances found in the gamma-ray yield curve in this region were the same as those seen in the elastic scattering of alpha particles from Ne^{20} . It is possible within the sum of the errors in the resonance energies and in the $\text{Na}^{23}(p,\alpha)\text{Ne}^{20}$ Q value to identify resonances 12, 14, and 15 with states observed in the elastic scattering of alpha particles by Ne^{20} . The angular distribution found for resonance No. 14 makes such an identification, how-

¹⁸ Baumann, Prosser, and Krone, Phys. Rev. **95**, 650 (1954).

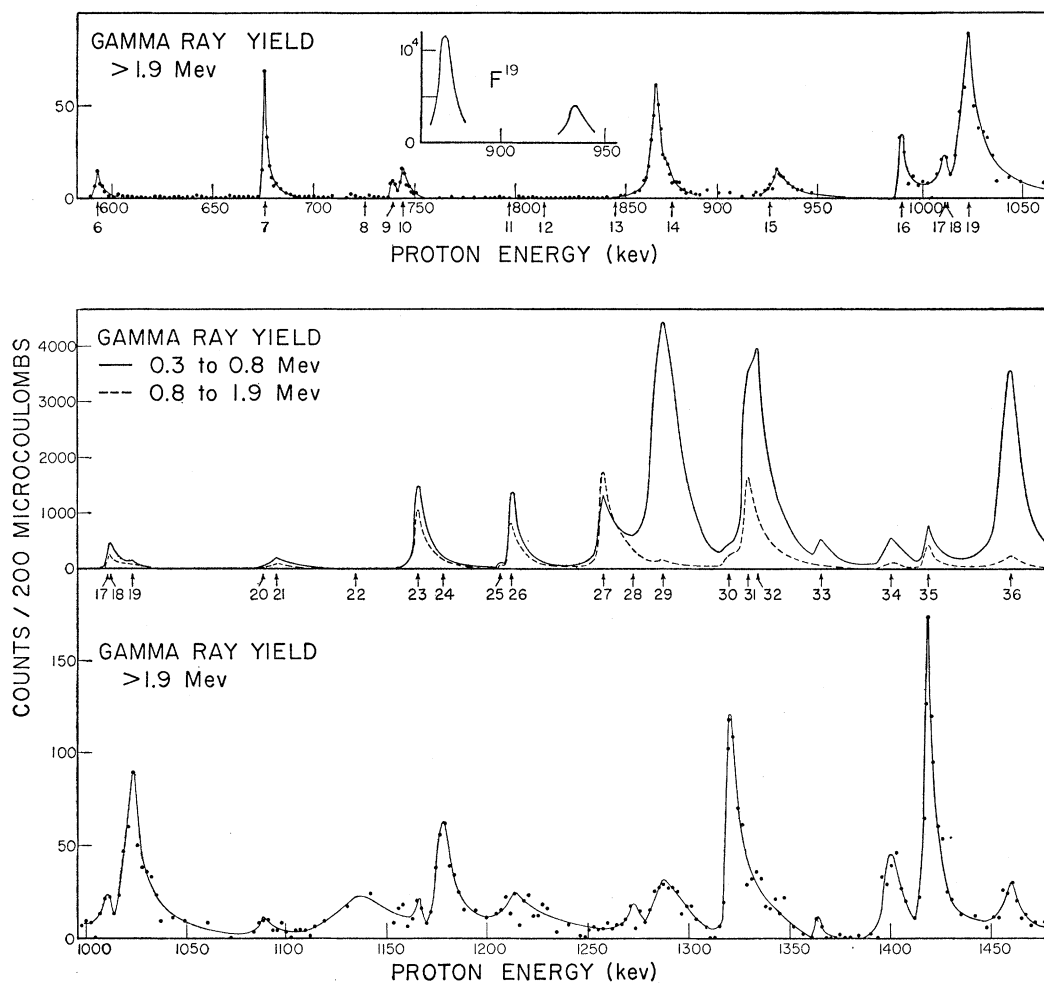


FIG. 2. Resonance curves showing the yield of gamma rays in the energy ranges indicated. Those gamma rays of energy greater than 1.9 Mev result from the reaction $Na^{23}(p,\gamma)Mg^{24}$, while those in the ranges 0.3 to 0.8 Mev and 0.8 to 1.9 Mev are indicative of the reactions $Na^{23}(p,p')Na^{23*}$ and $Na^{23}(p,\alpha')Ne^{20*}$, respectively. The insert shows the yield of gamma rays from the reaction $F^{19}(p,\alpha\gamma)O^{16}$. The resonances designated by the numbers include all those known in this region of the Mg^{24} compound nucleus.

ever, untenable. The subsequent work on particle emission¹³ confirms this conclusion.

Considerable care must be exercised in the interpretation of the gamma-ray yield curves obtained. It is well known that a monoenergetic gamma ray produces a complicated distribution of pulses which extends over the entire pulse-height spectrum. A high-energy gamma ray may therefore at times be recorded in a channel corresponding primarily to gamma rays of much lower energies. This difficulty is enhanced because for several resonances the cascade following capture proceeds through the first excited state in Mg^{24} at 1.37 Mev and the yield from this gamma ray will appear in the channel indicating alpha emission to the first excited state in Ne^{20} . A resonance occurring only for capture will, therefore, cause the appearance of a weak peak in the yield of low-energy gamma radiation, and a resonance in the α' channel will give the appearance of decay in

the p' channel as well. There is no unambiguous way to remove this effect without determining the spectrum at each resonance. All the yield in the two lower energy channels at proton energies less than 1 Mev appears to be attributable to this effect. It is felt that several of the weaker resonances reported by Stelson and Preston as decaying by p' and α' channels may decay primarily by capture. This would be difficult to establish by gamma-ray studies because of the very low yields.

The gamma-ray spectra obtained are shown in Fig. 3. The spectra from the $F^{19}(p,\alpha\gamma)O^{16}$ gamma rays and from a thick boron target are shown for comparison. The energy assignments for the various gamma rays are shown in Table I and the transitions believed to be represented by each are indicated in Fig. 1. Interpretation of the spectra was simplified by the known energies and transitions of the lower lying states, e.g., the 4.24-Mev state decays directly to the ground state while the

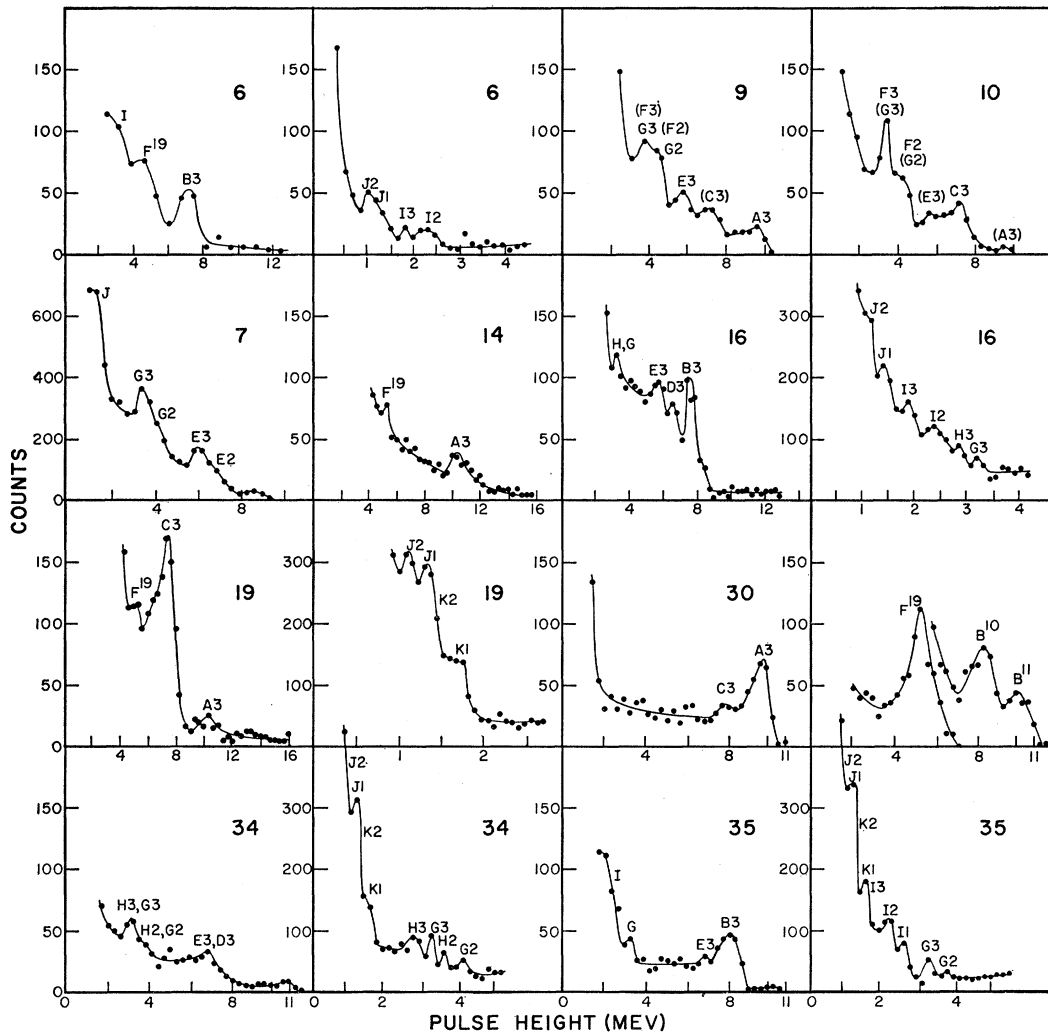


FIG. 3. Pulse-height distributions of the capture gamma radiation at the resonances indicated. The letters shown with the structure of the distributions refer to the gamma rays listed in Table I and are identified with the transitions shown in Fig. 1. The numerals following the letters indicate the detection process responsible for the structure, i.e., 1 indicates the full energy (photoelectric) peak, 2, the Compton edge and in some cases including pair formation with loss of one annihilation quanta, and 3, pair production with loss of both annihilation quanta. F¹⁹ indicates structure resulting from fluorine contamination of the target. Parentheses indicate structure arising from an adjacent resonance.

4.12-Mev state decays by cascade through the 1.37-Mev state. In several cases, particularly for the weaker transitions, the structure indicated is not statistically significant. For these cases, the interpretation has been based on consistency between higher and lower energy gamma rays and the known decays of the lower lying excited states. Where the structure of the spectra could be resolved, the gamma-ray energies are believed accurate to about 5%.

Angular distributions were obtained for six resonances. The angles for observation were chosen to follow the procedure suggested by Price¹⁹ to facilitate a least-squares fitting of the data to an expansion in

¹⁹ P. C. Price, *Phil. Mag.* 45, 237 (1954).

Legendre polynomials. The experimental points are shown in Fig. 4 together with the curves represented by the expression $W(\theta) = \sum A_i P_i(\cos\theta)$. The ratios of the coefficients A_i/A_0 and their probable error are given in Table II. Several of the coefficients, although statistically significant, were disregarded in the expressions plotted in Fig. 4. This was felt to be justified by visual comparison of the fit of the remaining terms to the experimental points. The probable errors, for both the points and the calculated coefficients, include only the statistical errors. Because of the reasonably good geometry and the smallness of the coefficients, no correction was made for the finite angle subtended by the counters.

TABLE I. Energies measured for the gamma rays shown in Fig. 3. The transitions believed to be represented by each are indicated in Fig. 1. Gamma rays *A* to *E* are initial transitions whose energies, therefore, vary with excitation energy.

Transition	Gamma-ray energy in Mev
<i>A</i>	11.1–11.5
<i>B</i>	8.1– 8.9
<i>C</i>	8.2– 8.8
<i>D</i>	7.1– 7.9
<i>E</i>	6.9– 7.4
<i>F</i>	4.2
<i>G</i>	4.2
<i>H</i>	3.8
<i>I</i>	2.8
<i>J</i>	1.4
<i>K</i>	1.6

DISCUSSION OF RESULTS

A rather abrupt change in the general appearance of the excitation curves is apparent at a proton energy of about 1 Mev. Below this energy capture is apparently the only important source of gamma radiation, while above this energy gamma radiation associated with particle emission from the compound nucleus rapidly becomes predominant. The apparent level density increases rapidly in this same region. Probably the principal reason for this transition is that the penetrabilities in the p' and α' channels, which are increasing rapidly at these proton energies, have become appreciably large in this region. At $E_p=1.0$ Mev and for s -wave emission, the penetrabilities for these two channels are about equal and only an order of magnitude smaller than that for d -wave decay in the p channel. Also, between proton energies of 1.0 to 1.5 Mev the penetrability for s -wave decay in the p channel changes from slightly less than to slightly greater than that for d -wave emission in the α channel. Therefore, at proton energies below 1 Mev, those compound states in the group with parity $(-1)^J$ will decay primarily by the α channel and those with opposite parity by the p channel.²⁰ For states with high spin values and with decreasing proton energy, capture will, of course, become more important, particularly for those states for which alpha emission is forbidden.

A study of the relative yields in the various channels can in principle lead to assignments of the spin and parity for the various levels. In practice, this is, however, difficult to do because the influence of the nuclear matrix elements cannot be disregarded and because the spin and parity of the first excited state in Na^{23} have so far not definitely been established.²¹ One may, however, reduce the possible choices in all cases. As mentioned above, those states which decay by the α channel must belong to the series with parity $(-1)^J$ while in turn the

²⁰ These conclusions would, of course, be partially invalidated by the operation of isotopic spin selection rules which could inhibit alpha emission where otherwise permitted.

²¹ R. W. Krone and W. G. Read, Bull. Am. Phys. Soc. Ser. II, 1, 212 (1956).

absence of the α channel would strongly favor the alternate series $-(-1)^J$. At those resonances showing capture radiation, a determination of the cascade may eliminate some possible choices, if one assumes that the gamma rays will carry not more than two units of angular momentum. Of the ten resonances at which the cascade spectrum was determined, only one does not decay directly to at least one of the first three excited states. One should expect, therefore, that those compound states that decay to the $4+$ state have spins larger than 2 and those that decay to the other two states have spins less than 4.

To place closer limits on the spin and parity assignments, it is necessary to consider the angular distributions of the reaction products. In the case of gamma radiation from an isolated resonance formed almost entirely by a single l value, a very convenient formalism is that proposed by Biedenharn and Rose.²² Because of the large number of parameters involved, e.g., channel spin, l value, multipole order, etc., it is impractical to tabulate all the possibilities here. The six compound states considered are essentially different in their characteristics and will therefore be discussed separately. In general, formation of a compound state of a given spin and parity will be assumed to be formed by the lowest compatible proton angular momentum. Where this criterion can be met with either channel

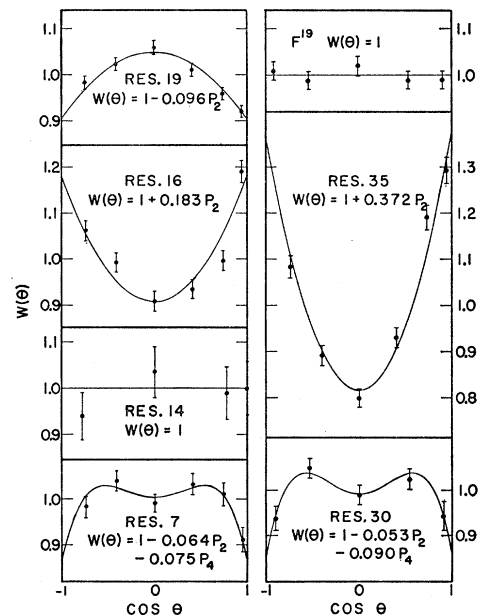


FIG. 4. Angular distributions of the initial gamma ray in the cascade following capture at the resonances indicated. The curves shown represent the expressions given in the figure. The disregarded terms and their probable errors are shown in Table II. The distribution labeled F^{19} is the distribution of the gamma rays from the reaction $F^{19}(p,\alpha\gamma)O^{16}$ at $E_p=935$ kev which was used as a check on the isotropy of the experimental procedure.

²² L. C. Biedenharn and M. E. Rose, Revs. Modern Phys. 25, 729 (1953).

spin, the ratio of the contributions from each will be treated as an adjustable parameter.

Resonance 35.—The principal cascade is through the $4+$ state. The resonance also shows decay through the α channel, restricting its spin and parity to the sequence $(-1)^J$. The angular distribution found agrees well with that expected for a $4+$ resonance decaying by $M1$ radiation to a $4+$ state, i.e., $A_2/A_0=0.393$, and cannot be fitted by a $3-$, $5-$, or $6+$ assignment. The appearance of a small $P_4(\cos\theta)$ term is explained by a small admixture of $E2$ radiation.

Resonance 14.—This resonance decays primarily through the $2+$ state at 1.37 Mev. The angular distribution of the 11.2-Mev radiation is isotropic within the probable errors. Since the decay by the α channel does not occur at this resonance, the spin and parity are restricted to the $0-$, $1+$, $2-$, and $3+$ sequence, unless isotopic spin selection rules suppress alpha emission. Isotropy is required for a $0-$ and $1+$ assignment. Isotropy may also be accounted for with a $2-$ or $3+$ assignment if one properly adjusts the ratio of the two channel spins, as well as the relative intensities of the magnetic dipole ($M1$) and electric quadrupole ($E2$) radiations. Because of the measured width of this compound state (8 ± 2 kev), a $3+$ assignment may, however, be ruled out, since d -wave protons would be required for its formation. No obvious choice can be made between the other possibilities on the basis of these data. Preliminary results from further work on elastic scattering¹³ indicate s -wave formation of the compound nucleus, agreeing with an assignment of $1+$ for this state.

Resonance 16.—The state decays primarily through the $4+$ state at 4.12 Mev, with strongly competing cascades through the states at 5.6 and 5.2 Mev. The angular distribution obtained can be fitted by a $3+$ assignment, assuming the state is formed through both channel spins and decays to the $4+$ state with both $M1$ and $E2$ radiation. It could also be fitted by either a $3-$ or $4-$ assignment, with, however, a mixture of $E1$ and $M2$ radiation required. From the similarity of the pulse-height spectrum to that of resonance 35 and from the narrowness of the resonance, the most tempting possibility is a $4+$ assignment, the decreased anisotropy being caused by the partial detection of

TABLE II. Experimental angular distribution coefficients and their probable errors obtained as a least-squares fit to the expression $W(\theta) = \sum A_i P_i(\cos\theta)$.

Resonance	A_1/A_0	A_2/A_0	A_3/A_0	A_4/A_0
7	0.007 ± 0.012	-0.064 ± 0.016	0.002 ± 0.019	-0.075 ± 0.021
14	0.032 ± 0.063	-0.069 ± 0.081		
16	-0.034 ± 0.016	0.183 ± 0.021	0.040 ± 0.025	0.045 ± 0.028
19	-0.010 ± 0.011	-0.096 ± 0.015	0.010 ± 0.018	0.011 ± 0.020
30	-0.007 ± 0.019	-0.050 ± 0.025	0.018 ± 0.030	-0.094 ± 0.033
35	-0.042 ± 0.016	0.372 ± 0.021	-0.033 ± 0.025	-0.043 ± 0.028
F19	-0.006 ± 0.019	-0.013 ± 0.025	-0.009 ± 0.030	0.036 ± 0.034

gamma rays from the competing cascades. The absence of decay through the α channel,¹³ as well as through the α' and β' channels, would be explained by the much smaller penetrabilities at this energy.

Because of the possibility of the detection of the alternate cascades and the lack of knowledge about the spins and parities of the 5.2- and 5.6-Mev states, a definite assignment cannot be made. On the basis of the decay spectrum, the best choices would seem to be $4\pm$.

Resonance 19.—With the primary decay to the $J=2$ state at 4.24 Mev, the angular distribution can be fitted by a $1-$, $2-$, or $3+$ assignment. The elastic scattering of protons¹³ is in agreement with a $2-$ assignment.

Resonance 30.—As long as the restriction to the consideration of only the lowest possible l -value in formation of a compound state is kept, the only assignment consistent with the angular distribution and the decay spectrum is $3+$. This requires contributions from both channel spins and a small admixture (at least 10%) of $E2$ radiation to $M1$.

Resonance 7.—The angular distribution at this resonance is the same within the probable errors as that of resonance 30, but the decay is through the state at 5.6 Mev whose spin and parity is not known. Until the properties of the 5.6-Mev state have been determined, there are too many alternatives leading to a fit of the data to attempt an assignment.